THE GABBROIC COMPLEX OF THE WESTERN OPHIOLITIC BELT, NORTHERN ALBANIA: AN EXAMPLE OF MULTILAYERED SEQUENCE IN AN INTERMEDIATE-SPREADING OCEANIC RIDGE°

Luciano Cortesogno*, **Laura Gaggero***, **Etleva Jaho***, **Michele Marroni****, **Luca Pandolfi**** and **Dode Shtjefanaku*****
(Presented at the Scientific Meeting of the G.L.O.M. in Firenze, February 24th, 1997)

* *Dipartimento di Scienze della Terra, Università di Genova, Italy*
** *Dipartimento di Scienze della Terra, Università di Pisa, Italy*
*** *Geological Enterprise of Rubik, Albania*

Keywords: *Gabbros, granulite facies, amphibolite facies, intermediate-spreading ridge. Mirdita, Albania.*

ABSTRACT

The paired ophiolitic belts of Albania are characterized by two contrasting stratigraphic and compositional signatures. Whereas the Eastern belt shows a thick sequence with IAT affinity, the Western ophiolites are characterized by a MOR-type sequence with a thickness not exceeding 4 km.

The western Mirdita ophiolite includes a mantle section overlain by a gabbroic complex consisting of cumulus dunites, melatroctolites, troctolites, norites, gabbros, diorites, Fe-Ti ox-gabbro-diorites with minor plagiogranites. The gabbroic complex, that everywhere shows a reduced thickness, is overlain by a sheeted dike complex with MORB affinity. The cumulus pile, from layered melatroctolites to diorites, is characterized by magmatic flow-related structures, such as foliation and lineation. The magmatic foliation is cut at low angle by mylonitic shear zones with high-T amphibolite facies assemblages. The shear zones are generally recognized in the lower-middle part of the gabbroic complex, whereas to the top of the sequence the brittle deformation prevails. The mylonitic shear zones are cut in turn by basaltic dikes and plagiogranitic bodies. The intrusion of basaltic dikes with IAT affinity represents a later magmatic event, that suggest a change in geotectonic environment.

On the whole, igneous and metamorphic features, as well as the thickness and composition of the basaltic cover on gabbros, support that the western belt of Albanian ophiolites representative of a ridge with intermediate spreading rate.

INTRODUCTION

A complete ophiolite sequence consists of several distinct layers that are also inferred in modern oceanic crust (Coleman, 1977). From the bottom up, the sequence consists of lherzolite and/or depleted harzburgites, layered ultramafic rocks, layered and isotropic gabbros, dike complex, effusive and sedimentary cover. However, important differences in the thickness and architecture of the ophiolite sequences can be recognized, mainly depending on their original setting in a fast or slow-intermediate spreading rate ridge. Reduced thickness of the sheeted dike complex, extensive deformation in the gabbroic complex, limited occurrence of the basaltic cover, gabbros intruding depleted mantle tectonites, periods of magmatic accretion alternated with amagmatic - expansion, higher degree of ridge segmentation, are some prominent features that characterize slow-spreading ridges, compared to fast ones (Karson and Dick, 1983; Boudier and Nicolas, 1985; Karson et al., 1987; Nicolas, 1988; Karson and Winter, 1992, Madge and Sparks, 1997).

Some features are very difficult to be recognized in the subducted complexes, due to the occurrence of ophiolite sequences as dismembered, generally deformed and metamorphosed slices in orogenic belts. By contrast, complete ophiolite sequences with well preserved transitions among the different layers are generally observed in the obducted sections of oceanic lithosphere.

In Albania, the Jurassic ophiolite sequences occur as fragments of oceanic lithosphere obducted from a Mesozoic Tethyan basin(s), located between the Eurasia and Adria plates. The Albanian ophiolites are divided in two, north-

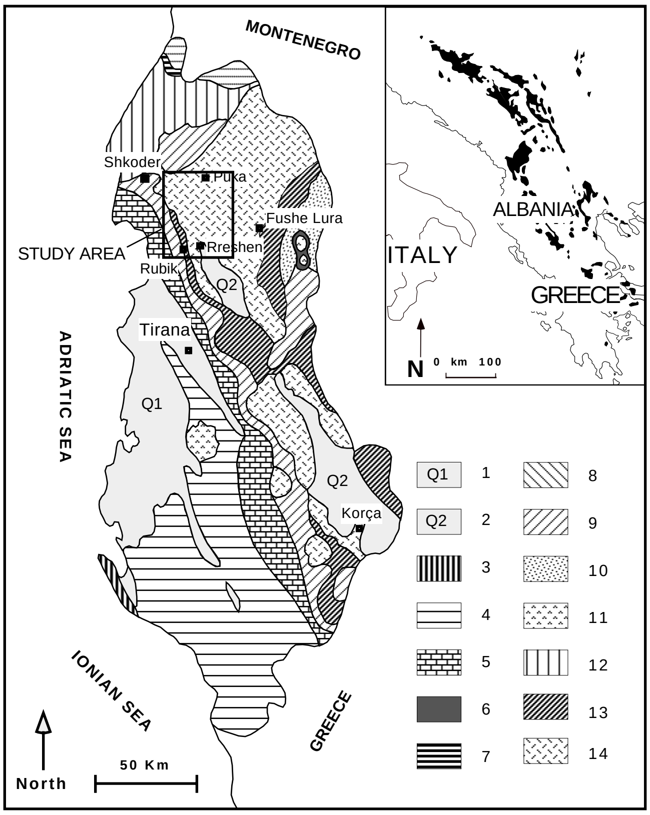

Fig. 1 - Geological sketch map of Albania. 1: Neogene-Quaternary deposits of the Periadriatic trough (Q1); 2: Neogene-Quaternary deposits of the Albano-Thessalian trough (Q2); 3: Pre-Apulian Zone; 4: Ionian Zone; 5: Kruja Zone; 6: Tertiary Flysch of Peshkopi Window; 7: Vermoshi Zone; 8: Gashi Zone; 9: Krasta-Cukali zone; 10: Korabi zone; 11: Permo-Trias gypsum; 12: Albanian Alps; 13: Rubik Complex; 14: Mirdita ophiolite nappe. The location of the area of Fig. 3 is boxed.

°Mirdita Ophiolite Project, contribution N°11 south trending belts, respectively the Western and the Eastern ones, showing different lithostratigraphic and petrologic features (Shallo et al., 1987; Shallo, 1992; 1994; Beccaluva et al., 1994; Bortolotti et al., 1996). Eastern ophiolites are interpreted as oceanic lithosphere derived from a Supra-Subduction Zone (SSZ) environment, whereas the Western ones as a lithosphere generated at a Mid-Oceanic Ridge.

The Western Albanian ophiolites provide an exceptional opportunity to study the different layers and their relationships compared to the modern mid-ocean ridge analogous. In this paper a set of geologic, stratigraphic and petrochemical data on the gabbroic complex of the Mirdita ophiolite is presented, and its emplacement and evolution in the lower oceanic crust is discussed.

GEOLOGICAL SETTING

Within the Alpine belt in the Eastern Mediterranean, Albania is interpreted as the linkage between the Dinarides and the Hellenides (Aubouin and Ndojaj, 1964; Aubouin et al., 1970). This sector is characterized by the occurrence of widespread ophiolitic sequences, remnants of a Jurassic Tethyan oceanic basin, located between the Adria (=Apulia) and Eurasia plates (Fig. 1). This Tethyan basin developed throughout a continental Mid-Late Triassic rifting and the following Early Jurassic spreading and drifting phases along the northern margin of the Gondwana. The Tethys oceanic lithosphere underwent a Middle Jurassic - Early Cretaceous subduction and obduction, followed by continent-continent collision. The suture zone formed during the progressive closure of the Jurassic Tethyan oceanic basin is represented by the Bosnian, Serbian, Albanian and Greek ophiolites (Robertson and Dixon, 1984, and quoted references).

In Albania, the Jurassic ophiolite sequence (i.e. the Mirdita Nappe) is thrust onto a west-verging stack of continental thrust sheets composed of sequences detached from the Adria margin (i. e. the Krasta-Cukali, Kruja and Ionian units). Between the continental units and the ophiolite nappe, an assemblage of continental and oceanic thrust sheets reported as Rubik Complex (Bortolotti et al., 1996 and quoted references) occurs.

The most exposed and best-preserved sequences occur in the Mirdita region, northern Albania (Fig. 1). On the basis of petrochemical data (Beccaluva et al., 1994), the Albanian ophiolites are subdivided into subparallel Western and the Eastern ophiolite belts, NNW-SSE trending with different stratigraphic, petrologic and geochemical features (Shallo et al., 1987; Shallo, 1992; Beccaluva et al., 1994).

The Western belt, that is thrusted by the Eastern one, includes an imbricate stack thrust sheets of ophiolites and the associated sedimentary sequence, (Kalur Cherts, Simoni Melange and Firza Flysch). Conversely, the Eastern belt is characterized by a huge, well preserved ophiolitic sequence from mantle ultramafic to sedimentary covers (ISPGJ-IGJN, 1982; 1983; 1990).

The Western belt shows an about 3-4 km thick sequence which mainly includes, from the bottom up, lherzolitic mantle tectonites, a gabbroic intrusive sequence, basaltic dikes and pillow lavas with high-Ti (MORB) affinity (Beccaluva et al., 1994 and quoted references), and Middle Jurassic radiolarites (Kalur Cherts). The occurrence of a typical sheeted dike complex is not reported. Although the Western belt is largely characterized by MOR-type ophiolites, volcanic sequences with intermediate MORB-IAT geochemical features, and very low-Ti basalt dikes are also found in this area. The intermediate-type volcanites are mostly represented by pillow basalts directly overlying the typical MORB ophiolite (Bortolotti et al., 1996).

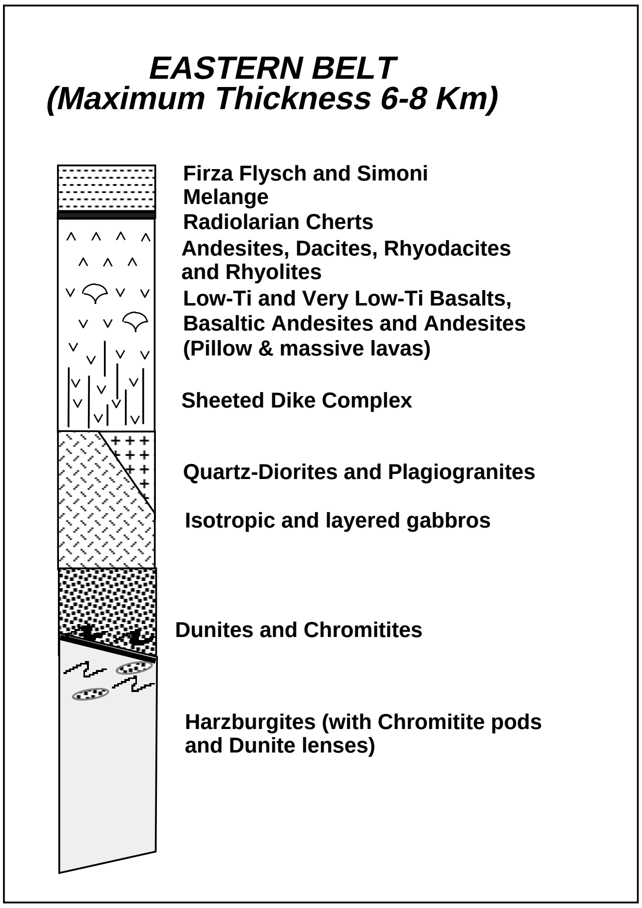

Fig. 2 - Generalized stratigraphical sequence for the Eastern ophiolitic belt (Modified after Bortolotti et al., 1996).

The Eastern ophiolite belt, 3-6 km thick, includes mantle harzburgites, mafic-ultramafic cumulates (chromite-bearing dunites, chromitites, dunites, websterites, gabbronorites, isotropic gabbros, quartz-diorites and plagiogranites), a well developed sheeted dike complex and a volcanic sequence of massive and pillow basalts, basalt andesites, andesites, dacites and rhyolites (Fig. 2). Boninitic dikes are also reported by Beccaluva et al. (1994). The sedimentary cover is represented by Middle Jurassic radiolarites (Marcucci and Prela, 1996 and quoted references). In the Eastern belt, the IAT geochemical characterization of basalt rocks supports an origin in a supra-subduction basin (SSZ ophiolites; Beccaluva et al., 1994).

As in the Eastern Mediterranean ophiolites (Spray et al., 1984), slices of metamorphic sole (ISPGJ-IGJN, 1982; 1983; 1990), represented by garnet-bearing amphibolites, coarse- to fine-grained amphibolites, garnet-bearing micaschists and garnet-bearing paragneisses (Carosi et al., 1996), occur at the base of the peridotite from Western and Eastern belts.

The ophiolites are unconformably overlain by a thick sedimentary sequence represented by the Late Jurassic- Early Cretaceous sedimentary melange and flysch, hereafter quoted as Simoni (=Mirdita) Mélange and Firza Flysch respectively, (ISPGJ-IGJN, 1982; 1983; 1990). Barremian-Senonian shallow-water deposits (ISPGJ-IGJN, 1982; 1983; 1990) cover

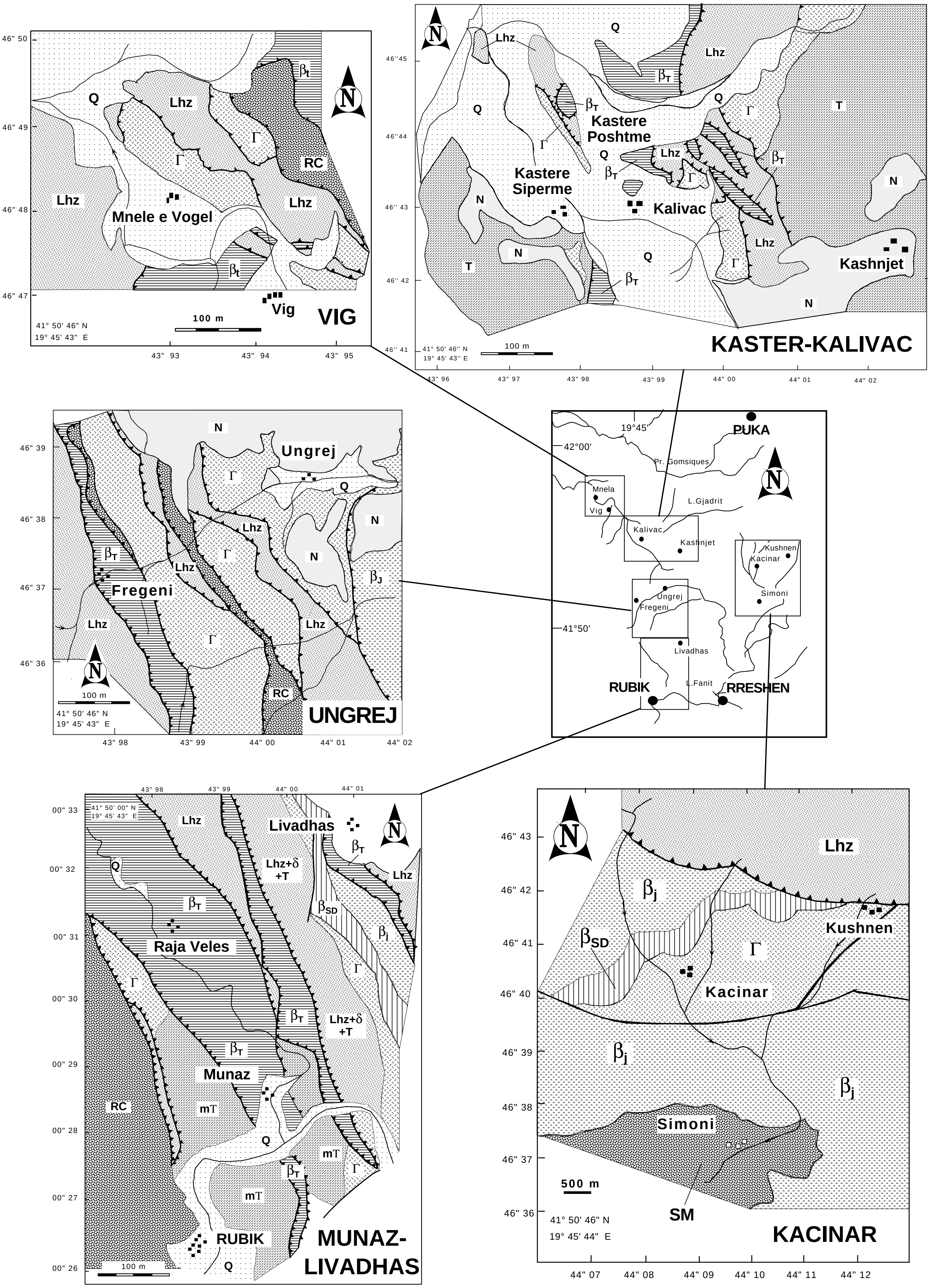

Fig. 3 - Geological maps of Ungrej, Kacinar, Munaz-Livadhas, Vig, Kaster - Kalivac areas Explanation: Lhz: lherzolites; d: dunites; G: gabbros; T: troctolites; mT: melatroctolites; bSD sheeted dike complex; bJ Jurassic basalts; RC: Rubik Complex; bT: Triassic basalts; SM: Simoni Mélange; N: Neogene sandstones and conglomerates; Q: Quaternary deposits. Fine line: primary relationships; heavy line: tectonic contacts (barbed) and faults.

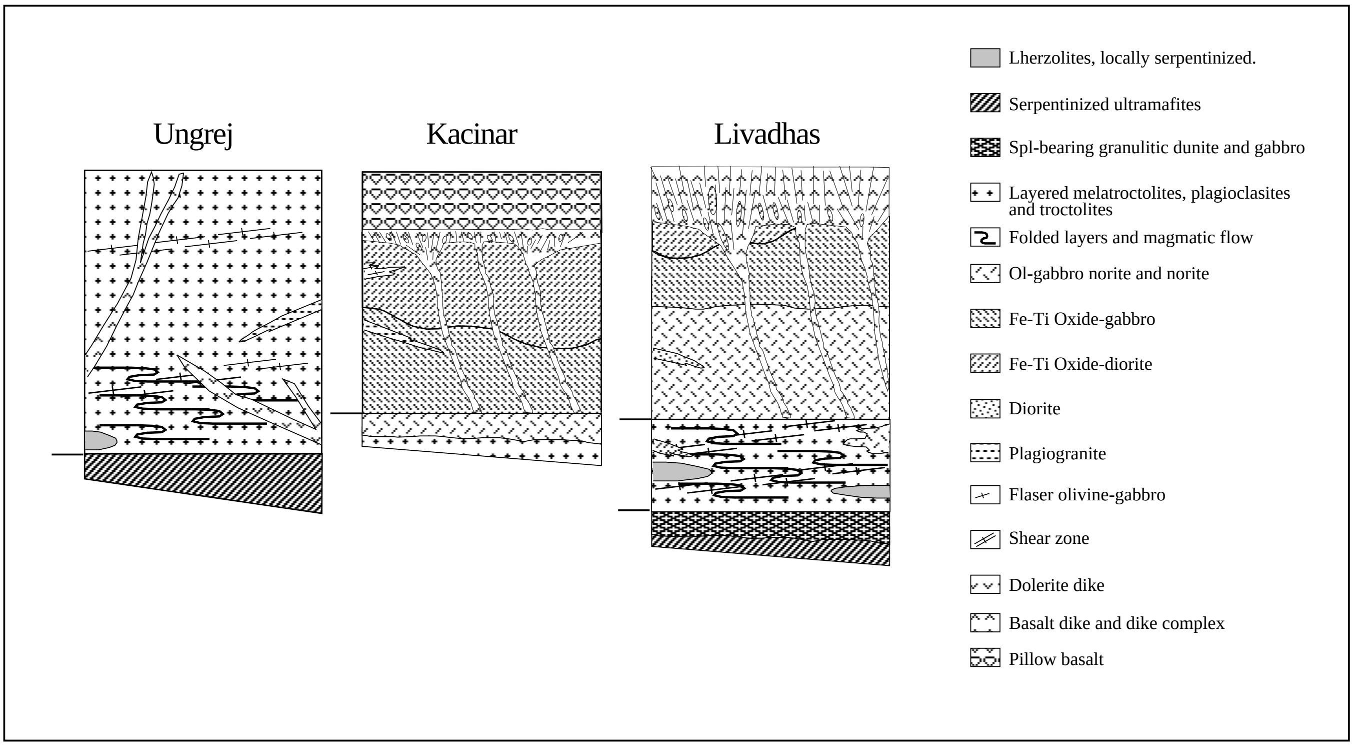

Fig. 4 - Inferred stratigraphy for Ungrej, Kacinar and Livadhas sequences (not to scale).

unconformably the sedimentary and ophiolitic sequences.

A more complete list of references in albanian is reported in Shallo et al., 1987; Shallo, 1992 and Beccaluva et al., 1994.

THE WESTERN MIRDITA GABBROIC COMPLEX

In spite of intense, orogenic brittle tectonics, the Western ophiolitic belt of the Mirdita region exhibits well preserved sections of a gabbroic complex, showing primary relationships with the mantle and the effusive complex. A complete reconstruction of these sequences was performed by detailed investigations along N-S aligned sections (Fig.3 and related stratigraphies of Fig. 4).

Ungrej

In the Ungrej area an east-dipping stack of slices made up of Triassic basalts, gabbros, lherzolites and Rubik complex crop out (Fig.3 and 4). Even if cut by thrust surfaces, the pristine stratigraphy of the gabbroic complex can be fully reconstructed.

The Ungrej section, representing the lower-middle part of the gabbroic complex, begins with cumulus melatroctolites, with decimetric to metric layers of leucotroctolites, wehrlites and Ol-gabbros, transitional to leucotroctolites. Metric tabular lherzolite bodies occur in the gabbroic rock; they likely represent xenoliths trapped in the crystal mush as a consequence of tectonic effects. Folded cumulates are overlain by a sequence of cumulitic troctolites, wehrlites with minor dunites and leucotroctolites. Isotropic troctolites and Ol-gabbros are prevalent at the top with minor interlayered melatroctolites.

Magmatic textures such as magmatic foliation, flow-induced folding (Fig. 6), boudinage and disruption of the layering (Fig. 7) are widespread in the lower part of the gabbroic complex. Locally, breccia textures develop as an effect of flow affecting the crystal mush and early solidified rock fragments (Figs. 8-9). Undeformed veins of gabbro and plagiogranite cut the visco-plastic flow (Fig. 10). The magmatic foliation is cut at low angle by mylonitic shear zones (Figs. 6 and 11) recrystallized into high grade amphibolite facies assemblage with clinopyroxene, plagioclase, red hornblende, and rare orthopyroxene.

Dolerite dikes cut the basal troctolites; they show chilled margins, and are devoid of plastic deformation, but are affected by widespread secondary blastesis of red hornblende at the expense of pyroxene and plagioclase. Basaltic dikes, devoid of important metamorphic effects, occur sparsely throughout the sequence.

Kacinar

In the Kacinar area, the gabbroic complex is thrust northwards by lherzolites slice and bounded southwards by east-west trending faults (Fig. 4).

The Kacinar section, representing the middle-upper part of the gabbroic complex, begins (Fig. 3) with cumulus melatroctolites grading to Ol-gabbronorites, with minor troctolite layers. Upwards, the transition to overlying Fe-Ti ox-gabbros occurs over some tens of metres, and is poorly exposed. The Fe-Ti ox-gabbros progressively grade to Fe-Ti ox-diorites and quartz - diorites with minor intercalations of olivine gabbronorites. Fe-Ti ox-gabbro-diorites show medium-grained hydiomorphic plagioclase with interstitial hornblende, with diffuse coarse to pegmatoid patches, where hornblende grows in parallel, radiating or dendritic aggregates (Fig. 12). Basalt dikes cut the sequence, spaced at the bottom and more frequent towards the top, where they constitute a sheeted dike complex with sparse gabbroic screens (Fe-Ti ox-gabbro to quartz-diorite). Fractures filled by green

Fig. 5 - Ungrej. Magmatic foliation, evidenced by layering, cut by low angle (<45°) metamorphic surface.

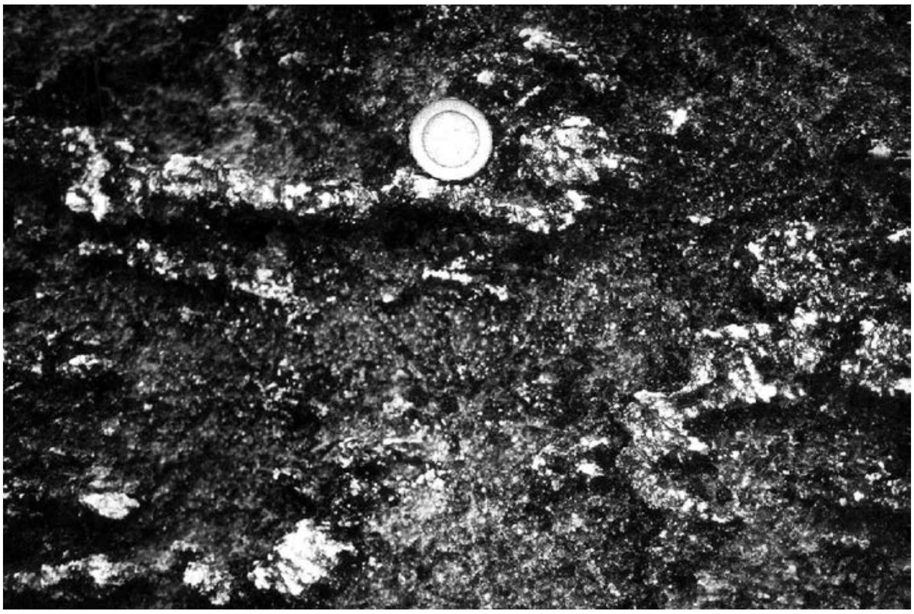

Fig. 6 - Ungrej. Syn-magmatic folding of a troctolite layer in melatroctolite.

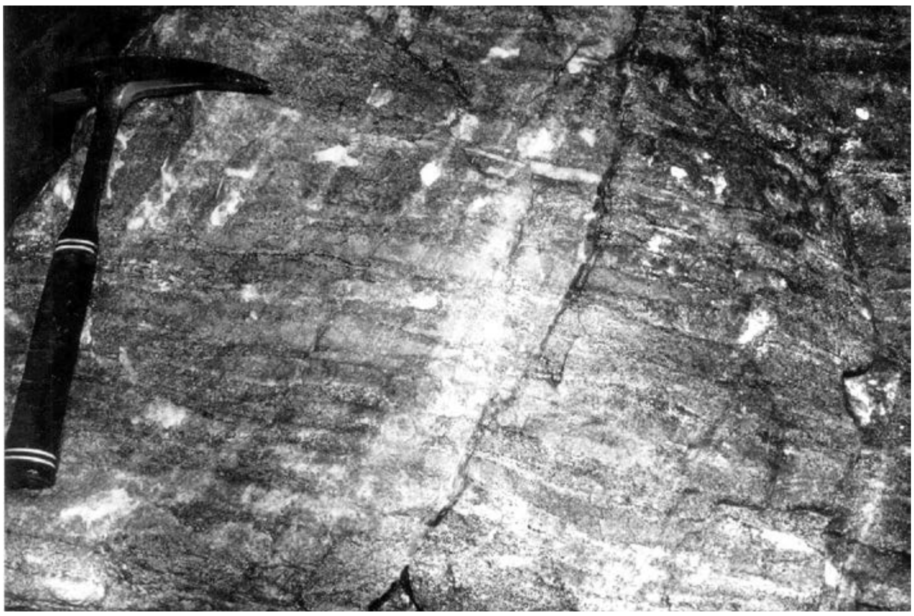

Fig. 7 - Ungrej. Layering in melatroctolites flattened and dismembered in magmatic environment.

Fig. 8 - Ungrej. Flattened and aligned troctolite fragments in melatroctolite matrix.

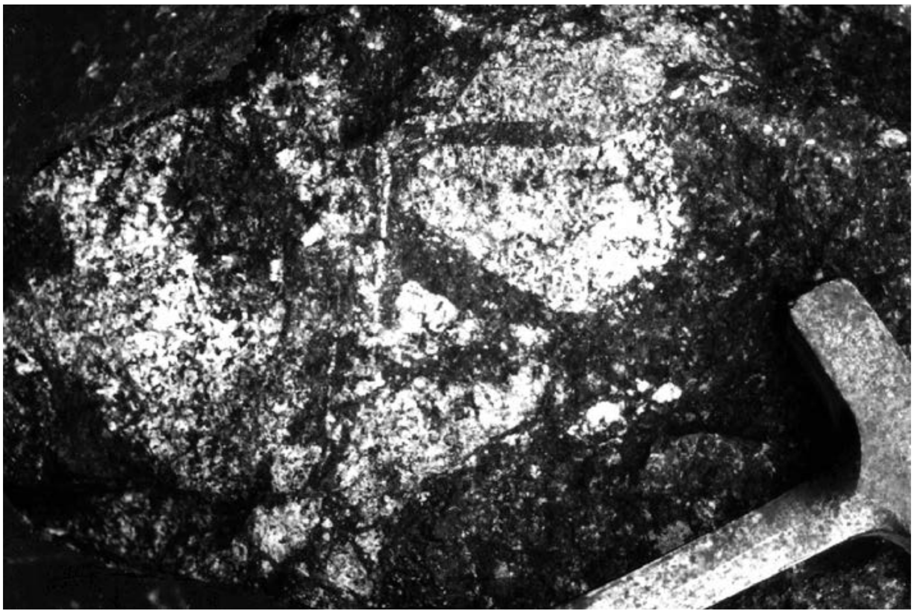

Fig. 9 - Ungrej. Detail of Fig. 10. Troctolite fragment fractured and filled by melatroctolite veinlets.

Fig. 10 - Ungrej. Undeformed vein of gabbro across layered and lineated melatroctolite.

Fig. 11 - Ungrej. High temperature banded metagabbro cut by amphibole - oligoclase and amphibole - albite veins.

hornblende diffusing in the host rock cut the screens and either lie parallel or cut the dikes. The section is topped by pillow basalts.

Munaz

In the Munaz area, a gabbroic complex occurs as a slice sandwiched between the Rubik Complex and Triassic basalts (Fig.3). The outcroping section represents a middle part of the sequence that begins with thick (200-400 m) melatroctolite cumulates, locally with millimetric layers of Cr-spinel, grading towards the top to troctolites with leucocratic lenses. They show adcumulus and heteradcumulus textures characterized by medium to pegmatoid grain size. Green hornblende veins occur sparsely. The boundary with overlying plagioclase - hornblende diorites is not exposed, but occurs in a few metres. The diorites (200-300 m thick) are characterized by flow foliation and lineation evidenced by the alignment of elongated prismatic hornblende.

Rubik

In the Rubik area the gabbroic complex occurs in the same tectonic setting as recognized in the Munaz area (Fig.3).

The Rubik intrusives (about 200 m thick), represent a lower - middle part of the gabbroic complex, which begins with melatroctolites and dunites, interbedded with lenses of olivine- and leucocratic gabbros. Pervasive plastic deformation and folding is associated with re-equilibration in amphibolite facies. Towards the top, melatroctolites with gabbro intercalations lack apparent deformation. Dikes of plagiogranites and tourmaline-bearing aplites, cut the lower part of the complex. Serpentinization of melatroctolites is associated with pervasive rodingitization of gabbros and minor alteration of plagiogranites.

Livadhas

Near Livadhas, the gabbroic complex occur as a slice between the Triassic basalts. However, in this area a complete stratigraphy of the ophiolite sequence from mantle ultramafics to basalts can be reconstructed.

At Livadhas, the ophiolite section includes (Fig. 3) a lower part represented by serpentinized lherzolites cut by gabbroic dikes affected by high grade metamorphic recrystallization. Above, spinel - dunites (at least 100 metres thick) are impregnated by a thick network of centimetric to decimetric veins of gabbroic composition (Fig. 13).

The gabbroic veins are deformed by isoclinal folds and re-equilibrated to a granulite assemblage with olivine, plagioclase, ortho- and clinopyroxene, and spinel. Locally, gabbro and Fe-Ti ox-gabbro dikes cut the dunites, and are affected by mylonitic shear zone developed under high grade amphibolite facies characterized by growth of plagioclase, clinopyroxene and red hornblende. Thrust surfaces separate the dunites from overlying cumulate dunites and melatroctolites pervasively deformed and recrystallized under high grade amphibolite facies. They include lenses (metres to decametres thick) of lherzolites, and are cut by undeformed dikes and pockets of Ol-gabbronorite. Upwards, adcumulus and heteradcumulus melatroctolites and interbedded gabbros show localized development of foliation associated with amphibolite facies overprint. The transition to the overlying gabbros is poorly exposed and occurs in some tens of metres. Thick, nearly isotropic, medium-fine grained, Ol-gabbronorites and gabbronorites, grade upwards to Fe-Ti ox-gabbro-diorites cut by rare fine-grained diorite dikes. At the top, a sheeted dike complex occurs, characterized by gabbroic screens, prevalent in the lower part, and by a network of dikes with different orientations of strike and dip.

Vig

In the Vig area, a sequence of thrust sheets including slices of the Rubik Complex, lherzolites, gabbros and Triassic basalts occur. In the main slice, cumulus troctolites overlying the mantle lherzolites, are cut by Fe-Ti ox-quartz diorite and plagiogranite dikes (Fig. 3).

Kaster-Kalivac

Near Kaster-Kalivac (Fig. 3), a stack of thrust sheets occurs. The main slice consists of a gabbroic complex represented by troctolites and melatroctolites, locally showing Cr-spinel layers, interlayered towards the top with olivine-gabbros. Fe-Ti ox-gabbros occur throughout the sequence as lenses and pockets.

On the whole, the investigated sections allow a reconstruction of the Western ophiolite sequence (Fig. 14) that includes a mantle section overlain by an gabbroic complex consisting of cumulus dunites, melatroctolites, troctolites,

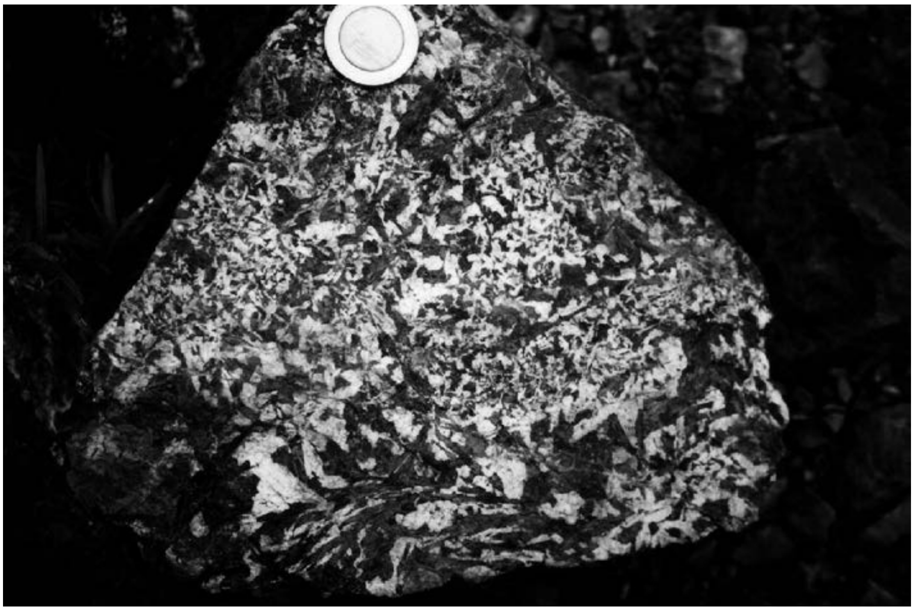

Fig. 12 - Kacinar. Coarse to pegmatoid bands and pockets of euhedral to radiating hornblende in Fe-Ti ox-diorite

Fig. 13 - Livadhas. Gabbroic and dunite layers isoclinally folded in granulite facies conditions.

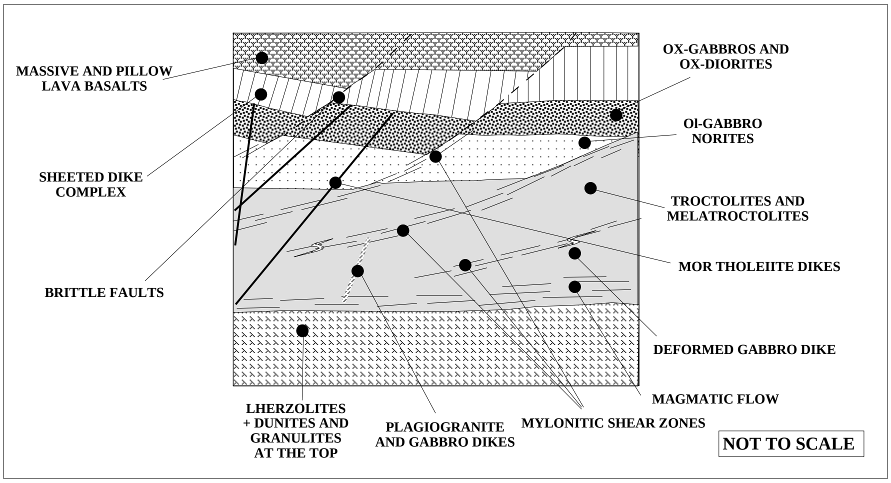

Fig. 14 - Sketch of the stratigraphy of Mirdita ophiolites and schematic relationship between magmatic and metamorphic events.

Table 1a - Major and trace element analyses of representative dunites, troctolites and olivine-gabbros from Kacinar, Rubik, Ungrej and Munaz-Livadhas.

Lithology	Plagioclase-Spinel dunite	Melatroctolite	Melatroctolite	Melatroctolite	Leuco-troctolite	Troctolite	Troctolite	Troctolite	Olivine-gabbro
Sample	AB 56	AB 5	AB 43	AB 75	AB 57	AB 45	AB 49	AB 74	AB 6
Provenance	Ungrej	Rubik	Ungrej	Munaz-Livadhas	Ungrej	Ungrej	Ungrej	Munaz-Livadhas	Rubik
Oxide wt%									
SiO2	36,98	36,02	38,12	34,03	40,10	37,44	46,74	45,51	37,38
TiO2	0,01	0,02	0,10	0,01	0,03	0,07	0,17	0,10	0,04
Al2O3	3,38	4,30	3,05	13,28	21,41	5,07	23,55	17,07	13,27
Fe2O3	9,37	8,04	8,30	4,28	4,04	9,35	3,48	6,94	5,96
MnO	0,14	0,12	0,13	0,07	0,05	0,15	0,06	0,10	0,08
MgO	41,51	38,58	38,37	23,31	18,18	35,91	10,23	16,67	25,81
CaO	1,22	1,94	2,38	15,05	9,58	1,98	11,55	8,04	8,91
Na2O	0,04	0,00	0,00	0,01	0,89	0,00	2,08	1,11	0,00
K2O	0,00	0,00	0,00	0,01	0,01	0,00	0,01	0,03	0,01
P2O5	0,00	0,00	0,00	0,00	0,00	0,00	0,00	0,00	0,00
L.O.I.	7,35	10,97	9,53	9,95	5,71	10,02	2,12	4,43	8,55
sum	100,00	99,99	99,98	100,00	100,00	99,99	99,99	100,00	100,01
Trace ppm									
Ba	<10	<10	<10	<10	<10	<10	<10	<10	<10
Co	89	78	77	45	38	82	17	45	44
Cr	2530	1940	1740	26	1135	3350	665	240	655
Cu	12	49	9	2	440	44	25	99	36
Nb	<3	<3	<3	<3	<3	<3	<3	<3	<3
Ni	1960	1855	1625	1130	400	1480	330	345	1180
Pb	3	3	b.d.l.	3	b.d.l.	4	3	2	b.d.l.
Rb	<5	<5	<5	<5	<5	<5	<5	<5	<5
S	280	610	995	1045	> 10700	1100	265	335	390
Sc	<5	<5	14	6	<5	<5	12	11	6
Sr	31	10	15	113	664	11	180	135	87
Y	2	2	4	2	2	2	3	4	2
Zn	46	40	44	22	16	51	17	41	28
Zr	3	3	7	3	3	3	8	3	3

Table 1b - Major and trace element analyses of representative gabbros and diorites from Kacinar, Rubik, Ungrej and Munaz-Livadhas.

Lithology	Metagabbro	Metagabbro	Gabbro	Granulitic metagabbro	Quartz-diorite	Olivine-gabbro	Olivine-gabbro	Olivine-gabbro	Olivine-gabbro
Sample	AB 20	AB 54	AB 84	AB 66	AB 52	AB 2	AB 14	AB 34	AB 78
Provenance	Kacinar	Ungrej	Munaz-Livadhas	Munaz-Livadhas	Ungrej	Rubik	Kacinar	Kacinar	Munaz-Livadhas
Oxide wt%									
SiO2	42,49	49,93	49,78	37,40	48,37	41,05	45,18	47,47	47,91
TiO2	0,08	1,03	0,77	0,04	1,19	0,16	0,14	0,13	0,30
Al2O3	3,23	18,46	16,37	13,67	20,70	9,64	20,28	21,80	17,80
Fe2O3	7,71	7,89	9,02	4,96	6,58	4,47	6,03	4,04	5,30
MnO	0,13	0,15	0,13	0,07	0,08	0,10	0,10	0,09	0,10
MgO	38,83	8,94	8,85	23,80	5,93	20,59	13,63	10,07	12,50
CaO	2,29	10,05	9,14	12,09	10,44	17,20	12,37	15,18	12,80
Na2O	0,03	3,14	3,20	0,12	4,64	0,07	1,01	0,99	1,43
K2O	0,01	0,04	0,13	0,02	0,17	0,00	0,01	0,00	0,03
P2O5	0,01	0,01	0,12	0,00	0,25	0,00	0,00	0,00	0,00
L.O.I.	5,20	0,38	2,47	7,82	1,65	6,71	1,26	0,21	1,84
sum	100,01	100,02	99,98	99,99	100,00	99,99	100,01	99,98	100,01
Trace ppm									
Ba	<10	<10	<10	11	23	<10	<10	<10	<10
Co	66	32	39	35	30	26	38	21	25
Cr	2775	240	330	640	31	2400	540	2150	1040
Cu	b.d.l.	28	14	33	6	73	85	85	69
Nb	<3	<3	<3	<3	<3	<3	<3	<3	<3
Ni	1985	181	114	1100	73	625	435	345	250
Pb	<5	b.d.l.	b.d.l.	3	<5	b.d.l.	b.d.l.	b.d.l.	b.d.l.
Rb	<5	<5	<5	<5	<5	<5	<5	<5	<5
S	350	295	39	640	20	410	1110	955	175
Sc	11	34	42	9	15	51	23	29	36
Sr	6	133	200	138	785	5	19	31	122
Y	2	14	25	2	22	7	6	6	10
Zn	43	44	32	22	27	23	33	19	26
Zr	4	16	60	3	107	5	5	4	14

Table 1c - Major and trace element analyses of representative Fe-Ti oxide gabbros and diorites from Kacinar.

Lithology	Fe-Ti oxide diorite	Fe-Ti oxide gabbro	Oxide quartz-diorite	Fe-Ti oxide diorite	Fe-Ti oxide diorite	Oxide quartz-diorite	Oxide quartz-diorite	Fe-Ti oxide diorite	Oxide quartz-diorite	Meta oxide-diorite	Fe-Ti oxide gabbro-diorite
Sample	AB 15	AB 16	AB 19	AB 23	AB 24	AB 25	AB 27	AB 28	AB 29	AB 31	AB 36
Provenance	Kacinar	Kacinar	Kacinar	Kacinar	Kacinar	Kacinar	Kacinar	Kacinar	Kacinar	Kacinar	Kacinar
Oxide wt%											
SiO2	38,28	44,78	45,15	53,12	57,58	47,41	50,20	53,07	49,07	51,63	47,16
TiO2	3,35	4,25	3,94	2,16	1,53	3,62	3,25	1,85	2,97	2,59	3,14
Al2O3	12,30	12,08	10,53	13,42	15,63	12,11	11,60	14,03	11,70	10,95	14,67
Fe2O3	21,56	18,54	19,73	13,95	10,39	21,53	20,01	15,07	18,93	17,57	15,29
MnO	0,23	0,28	0,26	0,18	0,12	0,28	0,25	0,17	0,28	0,26	0,21
MgO	8,43	7,64	8,19	3,62	2,32	4,60	4,18	3,88	5,49	5,02	6,74
CaO	12,41	8,13	8,25	6,63	3,95	5,91	4,92	5,11	6,28	7,06	8,43
Na2O	0,65	2,78	2,34	5,49	7,38	2,90	3,93	5,82	4,15	4,10	3,13
K2O	0,06	0,13	0,20	0,10	0,09	0,20	0,22	0,08	0,24	0,05	0,33
P2O5	0,26	0,35	0,38	0,53	0,24	0,73	0,85	0,39	0,54	0,51	0,22
L.O.I.	2,47	1,06	1,03	0,80	0,76	0,64	0,59	0,54	0,36	0,27	0,67
sum	100,00	100,02	100,00	100,00	99,99	99,93	100,00	100,01	100,01	100,01	99,99
Trace ppm											
Ba	<10	<10	40	<10	<10	<10	<10	<10	<10	<10	14
Co	99	99	95	60	67	107	100	60	87	77	68
Cr	21	30	34	17	6	18	15	15	34	27	63
Cu	51	57	37	48	32	25	11	33	21	11	33
Nb	5	4	4	5	4	8	7	6	6	5	2
Ni	b.d.l.	4	9	3	4	b.d.l.	b.d.l.	2	13	7	38
Pb	b.d.l.	4	3	b.d.l.	b.d.l.	2	5	3	3	4	2
Rb	<5	<5	<5	<5	<5	<5	<5	<5	<5	<5	<5
S	1530	2700	260	1120	695	1030	121	1300	425	38	1115
Sc	53	50	57	30	19	41	41	31	46	42	40
Sr	375	91	98	152	124	70	63	63	65	76	162
Y	63	50	51	93	96	108	116	123	83	98	35
Zn	225	165	82	75	55	64	66	62	92	86	82
Zr	170	165	160	314	>1120	417	420	625	282	310	87

Table 1d - Major and trace element analyses of representative plagiogranites from Rubik, Munaz-Livadhas, Kacinar and Ungrej.

Lithology	Meta-plagiogranite	Plagiogranite	Metagranite	Meta-aplite	Plagiogranite	Plagiogranite	Fe-Ti oxide plagiogranite	Fe-Ti oxide plagiogranite	oxide gabbro-diorite	Fe-Ti oxide diorite	Fe-Ti oxide diorite
Sample	AB 8	AB 9	AB 11	AB 12	AB 18	AB 30	AB 52'	AB 52'	AB 69	AB 76	AB 80
Provenance	Rubik	Rubik	Rubik	Rubik	Kacinar	Kacinar	Ungrej	Ungrej	Munaz-Liv.	Munaz-Liv.	Munaz-Liv.
Oxide wt%											
SiO2	77,61	67,04	65,89	75,56	44,93	77,49	65,75	65,75	42,37	49,45	47,89
TiO2	0,11	0,14	0,05	0,05	0,18	0,21	0,74	0,74	0,12	0,53	0,59
Al2O3	12,94	19,13	17,53	14,44	19,01	11,71	14,13	14,13	22,42	14,22	18,68
Fe2O3	0,90	0,90	0,63	0,45	7,04	2,57	6,25	6,25	6,41	9,51	7,41
MnO	0,02	0,01	0,01	0,01	0,12	0,02	0,09	0,09	0,12	0,12	0,12
MgO	0,23	0,63	0,27	0,00	14,69	0,36	2,64	2,64	7,77	11,09	10,61
CaO	0,75	0,29	3,86	0,21	12,38	0,56	3,98	3,98	16,33	9,19	8,52
Na2O	6,71	11,31	10,74	5,16	0,82	6,53	4,75	4,75	0,52	3,71	2,63
K2O	0,19	0,01	0,17	3,77	0,01	0,03	0,22	0,22	0,18	0,05	0,10
P2O5	0,03	0,07	0,04	0,06	0,00	0,02	0,40	0,40	0,00	0,04	0,05
L.O.I.	0,52	0,46	0,81	0,29	0,82	0,49	1,05	1,05	3,78	2,07	3,39
sum	100,01	99,99	100,00	100,00	100,00	99,99	100,00	100,00	100,02	99,98	99,99
Trace ppm											
Ba	50	<10	30	38	<10	<10	40	40	23	<10	<10
Co	39	12	5	25	39	13	23	23	26	45	34
Cr	b.d.l.	b.d.l.	3	b.d.l.	870	b.d.l.	3	3	115	26	195
Cu	b.d.l.	b.d.l.	b.d.l.	b.d.l.	57	15	180	180	4	2	58
Nb	7	9	10	19	2	3	2	2	2	2	2
Ni	b.d.l.	b.d.l.	b.d.l.	b.d.l.	550	b.d.l.	b.d.l.	b.d.l.	147	65	151
Pb	14	3	21	8	b.d.l.	2	2	2	2	b.d.l.	3
Rb	<5	<5	<5	110	<5	<5	<5	<5	<5	<5	<5
S	19	19	20	19	945	33	33	33	335	25	72
Sc	<5	<5	<5	5	24	<5	27	27	53	42	34
Sr	56	24	40	8	24	37	106	106	210	108	120
Y	24	29	24	18	7	22	70	70	5	14	16
Zn	5	<5	<5	5	36	13	19	19	20	38	44
Zr	64	99	50	28	8	425	225	225	4	32	29

Table 1e - Major and trace element analyses of representative basalts and dolerites from Kacinar, Ungrej and Munaz Livadhas.

Lithology	Aphyric basalt	Basalt	Basalt dike	Basalt dike	Basalt	Basalt dike	Basalt dike	Metabasalt	Basalt dike	Basalt dike	Basalt dike	Metabasalt	Metadolerite	Metadolerite
Sample	AB 16'	AB 21	AB 22	AB 35	AB 38	AB 39	AB 40	AB 41	AB 51	AB 53	AB 79	AB 81	AB 82	AB 83
Provenance	Kacinar	Kacinar	Kacinar	Kacinar	Kacinar	Ungrej	Ungrej	Ungrej	Ungrej	Ungrej	Munaz-Livadhas	Munaz-Livadhas	Munaz-Livadhas	Munaz-Livadhas
Oxide wt%														
SiO2	47,51	46,75	46,39	48,07	48,09	51,83	52,62	54,48	48,55	44,55	46,87	49,71	49,72	48,96
TiO2	0,63	0,62	0,63	0,96	1,26	0,24	0,24	0,24	1,20	1,87	0,90	1,72	1,61	1,10
Al2O3	16,15	16,83	16,92	16,07	15,31	14,22	13,85	15,33	15,99	14,78	16,11	14,92	15,85	16,95
Fe2O3	9,88	9,23	9,10	10,90	12,61	12,08	11,74	10,30	10,67	16,45	9,00	10,90	10,07	8,80
MnO	0,16	0,15	0,15	0,18	0,20	0,19	0,18	0,16	0,19	0,22	0,17	0,18	0,15	0,14
MgO	11,03	11,56	11,73	9,08	8,55	8,93	8,78	7,69	9,08	8,90	10,89	8,30	8,65	9,53
CaO	10,75	10,48	10,21	11,15	10,10	6,22	6,53	5,58	9,72	6,92	10,87	8,73	9,20	9,88
Na2O	1,80	1,80	1,92	2,13	2,49	4,07	4,06	4,82	2,89	3,04	2,18	3,74	3,14	2,73
K2O	0,05	0,09	0,07	0,07	0,16	0,08	0,08	0,10	0,16	0,02	0,03	0,12	0,17	0,14
P2O5	0,01	0,02	0,02	0,04	0,06	0,00	0,01	0,00	0,11	0,32	0,04	0,19	0,22	0,12
L.O.I.	2,03	2,48	2,86	1,36	1,17	2,13	1,92	1,28	1,43	2,92	2,03	1,50	1,21	1,64
sum	100,00	100,01	100,00	100,01	100,00	99,99	100,01	99,98	99,99	99,99	99,09	100,01	99,99	99,99
Trace ppm														
Ba	<10	<10	<10	<10	<10	<10	<10	<10	<10	<10	<10	<10	<10	<10
Co	50	44	48	52	58	53	54	46	48	72	46	48	60	48
Cr	480	420	435	380	145	145	130	92	285	131	405	240	250	335
Cu	89	66	66	67	62	54	22	230	74	42	90	94	12	22
Nb	2	2	2	2	2	2	2	2	2	2	2	3	2	2
Ni	170	230	230	11	78	32	29	22	70	87	176	98	131	160
Pb	3	b.d.l.	b.d.l.	3	b.d.l.	2	b.d.l.	b.d.l.	3	b.d.l.	b.d.l.	b.d.l.	3	2
Rb	4	4	4	4	4	4	4	4	4	4	4	4	4	4
S	365	650	690	720	1525	122	79	465	1870	68	200	48	23	32
Sc	37	30	31	39	41	59	59	51	38	39	31	40	39	37
Sr	45	63	66	63	51	94	103	142	132	84	83	136	135	146
Y	22	21	21	28	35	9	8	9	31	61	24	39	41	26
Zn	96	64	64	79	91	44	42	51	55	160	60	53	48	36
Zr	18	18	17	42	55	11	11	13	82	165	44	138	136	83

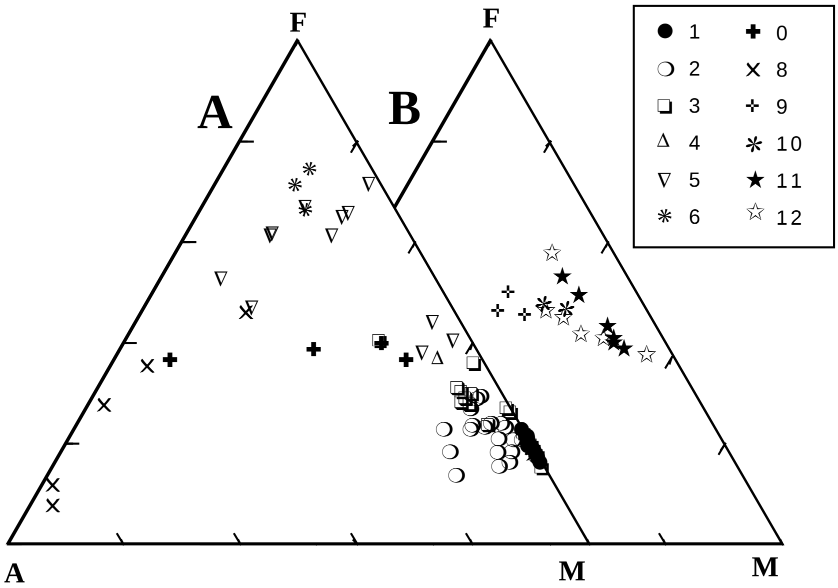

Fig. 15 - AFM diagram for the Mirdita gabbroic (A) and basaltic (B) rocks. Symbols: 1: Melatroctolites; 2: Troctolites and Ol-gabbros; 3: Gabbronorites and norites; 4: Ol-oxide gabbros; 5: Fe-Ti ox-gabbros and Fe-Ti ox-diorites; 6: Fe-Ti ox-quartz diorites; 7: Quartz-diorites; 8: Plagiogranites. 9: Ungrej dolerites; 10: Ungrej high Ti basaltic dikes; 11: Munaz Livadhas dike complex; 12: Kacinar dike complex.

norites, gabbros, Fe-Ti ox-gabbro - diorite. At the bottom of the cumulus sequence, dikes are rare and become more frequent upwards; to the top, they form a sheeted dike complex with minor gabbro screens. The whole gabbroic complex shows magmatic structures as lineation, foliation, banding and folding, cut at low angle by mylonitic shear zones developed under amphibolite facies conditions. The mylonitic shear zones are widespread at the base of the gabbroic complex and rarer towards the top, where the brittle deformation prevails.

PETROCHEMICAL FEATURES

Analytical techniques

Whole rock major and trace element abundances for gabbros and basalts of the Mirdita ophiolite were determined by XRF techniques using a Philips PW 1480 XR spectrometer at the Dipartimento di Scienze della Terra, Università di Genova. Intensities were elaborated according to Franzini et al. (1975) and Leoni and Saitta's (1975) methods. Loss on ignition (LOI) was determined by the gravimetric method. Representative compositions of plutonites and basic effusives are in Tab. 1.

The gabbroic complex

The investigated gabbroic complex represents a complete tholeiitic gabbroic intrusion controlled by fractionation and accumulation. The relationships between crystallization and accumulation with chemical compositions are obvious in a AFM diagram (Fig. 15A). In melatroctolites and rarer dunites, the composition reflects the segregation and growth (adcumulus and heteradcumulus) of olivine (Fo≥ 88 mole%) and subordinate An-rich plagioclase (An≥ 90 mole %). In troctolites the M/F ratio is constant, whereas higher A evidences both a modal increase of plagioclase up to leucocratic compositions, and a moderate decrease of An content.

The thick layers of gabbronorites and norites show decreased M/F, with intermediate A, as a consequence of pyroxene crystallization and accumulation in mesocratic compositions. The higher levels in the cumulus sequence, strongly differ for the crystallization of hornblende instead of pyroxenes, and for the appearance of Fe-Ti oxides, sometimes coexisting with Fe-rich olivine. In the AFM diagram this corresponds to a decrease of M/F, whereas no evident A increase results, in spite of higher Ab/An in plagioclase; this is a consequence of the melanocratic character of these rocks. The transition between Fe-Ti ox-gabbro and Fe-Ti ox-diorites is not obvious in the field, conversely, in the AFM diagram, a compositional gap expressed by a sharp difference in M/F, separates gabbroic from dioritic compositions, depending on increased oxides/femic silicates ratio. The highest F corresponds to Fe-Ti ox-quartz - diorites that show low modal quartz. The progressive parallel decrease of femic phases and of anorthite in plagioclase is evidenced by the shift of compositions towards A that marks the transition to plagiogranites.

A different trend is shown by (Fe-Ti oxide free) quartz-diorite dikes, characterized by constant F/M, that expresses the homogeneous composition of the femic phases (hornblende), and by increasing A, that corresponds to the transition from mesocratic to leucocratic compositions.

The basaltic dikes

The sheeted dikes at Kacinar and Livadhas, and basaltic dikes at Ungrej show typical tholeiitic trend on the AFM diagram and high-Ti MOR affinity in the Ti/Cr vs. Ni correlation (Beccaluva et al., 1983, Fig. 16). The dikes have an overall MORB-type pattern in Rock/MORB normalized spiderdiagram (Fig. 17), with slightly higher Rb and Ba. In addition, a La and Gd positive anomaly and Ce and Dy negative anomaly occurs at Ungrej and Livadhas, in contrast with a negative La anomaly in Kacinar basalts.

TiO2 wt% ranges between 0.62-1.26 (Kacinar), 1.2-1.87 (Ungrej), and 0.90-1.72 (Livadhas); Zr ppm between 17-55 (Kacinar), 82-165 (Ungrej), and 44-182 (Livadhas); Y ppm between 21-35 (Kacinar), 35-61 (Ungrej), and 26-41 (Livadhas). These values are consistent with MORB abundances, and indicate a progressive enrichment in incompatible elements from present N to S.

Compared to basaltic dikes, dolerites intruding the base of the gabbro sequence at Ungrej, show higher alkali abundance (Fig. 15B) and lower Ni abundances, so that they correspond to IAT and very low Ti basalt (Fig. 21). They also

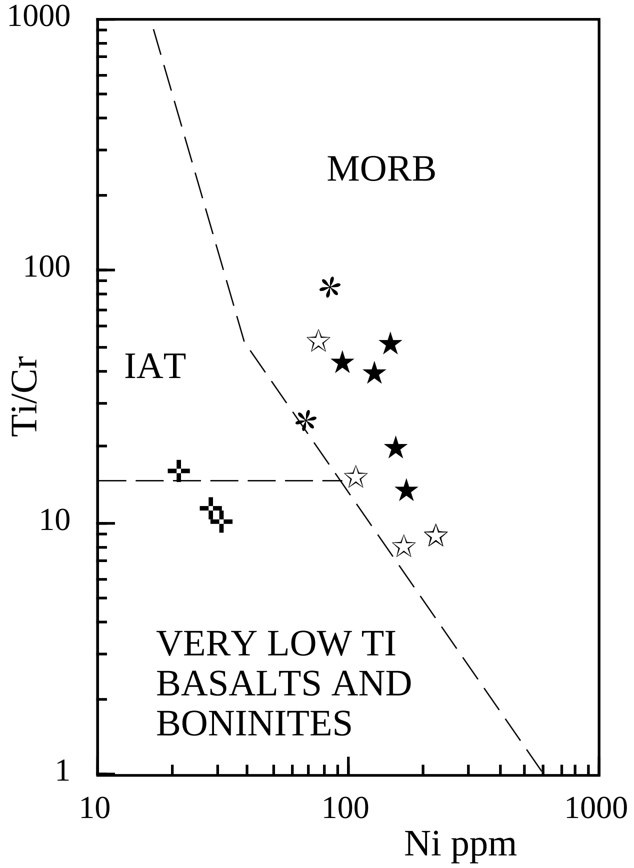

Fig. 16 - Ti/Cr vs. Ni discrimination diagram (after Beccaluva et al., 1983) for Ungrej dolerites and Munaz Livadhas and Kacinar dike complexes; symbols as in Fig. 15.

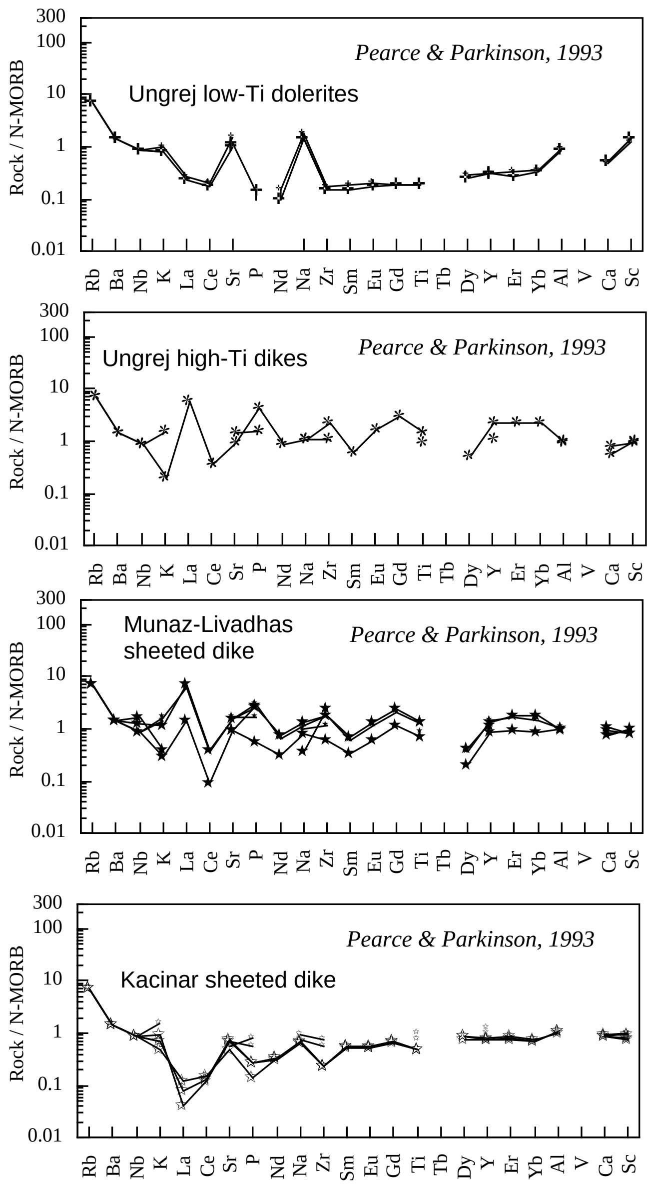

Fig. 17 - Rock/MORB spidergram for basalts. Symbols as in Fig. 15.

evidence average patterns lower than MORB (Fig. 17), except for Rb, Ba, K, Sr, Na, Al and Sc.

DISCUSSION AND CONCLUDING REMARKS

The western Mirdita gabbros can be, on the whole, ascribed to a unitary genetic model, although important differences occur locally; the emplacement of parental liquids, the crystallization of gabbros and the tectonic overprints, scan the timing of the evolution of the ridge segment. The first recorded episode, represented by dunites impregnated by gabbro veins, occurs likely during the early uplift phase of the lherzolites. At the moment, data are insufficient to assess if dunites are i) early cumulates (e.g. Flinn, 1996), ii) refractory of an important extraction of melt (Boudier and Nicolas, 1977), ii) replacive dunites (Cannat and Lécuyer, 1991; Ceuleneer and Rabinowicz, 1992; Kelemen et al., 1997). The hypotheses ii) and iii) can better account for the high Cr content in dunite spinels (100Cr/Cr+Al > 80). Spinels in granulitic metagabbros have higher Al contents and decreasing Cr/Mg, and strongly differ from the high Al chromites in cumulitic melatroctolites (unpublished data). They likely originate by fractionation from the liquids impregnating the dunite, and re-equilibration under granulite - facies conditions.

The melting and channeling of gabbroic veins is considered associated with a plastic strain that played a prominent role in the drainage of small melt pools, and occurred in the plagioclase lherzolite facies (as, e.g. at Lanzo and Trinity). A sequence of lherzolites cut by plagioclase-rich gabbro veins and tabular dunite pods can be compared with the Trinity ophiolite, where these features are observed 200-300 metres below the petrological paleo-Moho (Quick, 1981). However, at Livadhas an important ductile flow likely sub-horizontal, associated with reconstitution in granulite facies, post-dates the dunites and the gabbro veins. The dunite and gabbroic granulite layers represent a transition level generated at the boundary between an upwelling lherzolite mantle, and the lithospheric magma chambers.

The overlying cumulus complex is characterized by a tholeiite-type vertical fractionation from i) olivine ± plagioclase and rare Al-Cr bearing spinel cumulates through ii) the crystallization of scarce troctolites and prevalent Ol-norite and gabbro norites, to iii) the precipitation of Fe-Ti oxides in hornblende gabbros and diorites. The more evolved compositions are represented by quartz - bearing hornblende diorites and plagiogranites, mostly as dikes and pockets.

During the fractional crystallization of the gabbroic complex, tectonic events developed in an ocean floor environ-

Table 2 - Timing and nature of events in the Mirdita ophiolite.

TIME	GEODYNAMIC ENVIRONMENT	TECTONICS EVENTS	MAGMATIC EVENTS	METAMORPHISM
↑	SUPRA-SUBDUCTION SETTING (?)		IAT dolerite dikes	Amphibolite facies water diffusion
		Fracturing	MOR basaltic dikes and sheeted complex	Greenschist and low-T amphibolite facies
		Tectonic elision of the chamber(s) lid Brittle fracturing on top Shear surfaces at depth		Water diffusion Low-T amphibolite facies on top High-T amphibolite facies at depth
T I M E	OCEANIC BASIN	Visco-plastic flow in the crystal mush	Fractional crystallization and cumulus	
		Opening of magmatic chambers	Emplacement of MORB liquids	
		Foliation and folding		Granulite facies
		Hydrofracturing	Gabbro veining	
			Replacive (?) dunites	

ment, recorded by magmatic foliation and compositional layering, frequent in basal melatroctolites, and in the cumulus pile up to the diorites. At the base, magmatic foliation and lineation are associated with folding, boudinage and necking of the pre-existing layering.

In turn, the magmatic foliation is cut at low angle by mylonitic shear zones with high-T amphibolite facies assemblages. Shear zones are rarely developed towards the top of the sequence. In the uppermost part of the gabbroic complex as well as in the sheeted dike complex, faults and hornblende-filled veins are widespread.

MOR basalts and diorite - plagiogranite dikes cut the mylonitic shear zones, but no evidence allows to assess the relative timing of intrusion. The succession of events is synthesized in Tab. 2.

On the whole, the structural features recognized in the gabbroic complex from Western Mirdita ophiolites reveal the occurrence of a long-lived, continuous extensional tectonics during the opening of temporary magmatic chambers, and during the cumulus phases. The reduced thickness of the whole gabbroic complex can be regarded as the result of such regime. This is also suggested by the occurrence of incomplete sequences, as in the Munaz section, where part of the gabbroic complex was probably stripped off along a low-angle shear zone during the extensional tectonics, and diorites were emplaced with textures of syn-tectonic flow directly above cumulus melatroctolites.

Whereas in the lower part of the gabbroic complex the extensional tectonics results in low angle dipping shear surfaces, in the upper part, it is accomodated by brittle deformation as faults and hornblende-filled veins, preceding and coeval to the emplacement of sheeted dikes. The elision of such cover necessarily occurred during the extensional tectonics. The gabbro screens intruded by the basalt dikes show coarse hypidiomorphic textures, therefore indicating the presence of an older confining cover. The basaltic dikes represent a third magmatic event post-dating the main extensional tectonics.

On the whole, the stretched oceanic crust represented by western ophiolite sequence of Albania underwent episodic magmatic events during extensional tectonics, as already envisaged in some ophiolite sequences and in their modern analogues at slow and intermediate spreading ridges (e.g. Varga and Moores, 1985; Alexander and Harper, 1992).

The sheeted dikes at Kacinar and Livadhas, and basaltic dikes at Ungrej show typical MOR tholeiite features. Minor differences between the trends of Kacinar and Livadhas complexes express the composition of different magma batches.

The dolerites with IAT affinity intruding the basal melatroctolite level represent a further magmatic event. The well developed chilled margins are consistent with the emplacement in a cooled cumulus pile; on the other hand, the development of secondary hornblende evidences water diffusion under high grade amphibolite conditions coeval with the dike emplacement. Thus, it can be envisaged that i) relatively high temperatures were preserved at the bottom of the gabbroic complex until the intrusion of the dolerites, or, ii) it is possible that the water diffusion, the dolerite emplacement and the thermal increase represent a separate geodynamic event. The IAT geochemical affinity also characterizes part of basaltic effusives (Bortolotti et al., 1996 and unpublished data); this makes problematic the interpretation of the relationships between the Western and the Eastern albanian ophiolites; anyway, a possible implication of MOR ophiolites in an arc-type setting can be inferred.

On the whole, the stratigraphy of the gabbroic complex strongly suggests that the western Mirdita ophiolite represents an ocean crust section originated in a mid - ocean ridge, evolving to off-axis environment. The crustal thickness not exceeding 700 m, the occurrence of plastic deformation represented by shear zones, the omissions within the gabbroic complex, and the delamination of the cover above gabbros, support that extensional tectonics was effective during the spreading. However, i) the presence of large gabbroic intrusions, and of a sheeted dike complex ii) the lack of ophiolitic breccias, and iii) of widely serpentinized ultramafites directly exposed at the seafloor, iv) the moderate development of ductile and brittle deformation associated with amphibolite facies metamorphism, v) the virtual absence of a hydrothermal, low-grade, off-axis metamorphism in gabbros (e.g. compared to MARK area, Gaggero and Cortesogno, 1997; and to Northern Apennine ophiolites, Cortesogno and Lucchetti, 1982), vi) the occurrence of a probably continuous layer of pillow basalts, make the Western Mirdita ophiolite different from slow spreading ridges, to which it has been assimilated (Boudier et al., 1997). By contrast, the stratigraphy, the lithospheric thickness, the deformational features, and the character of seafloor alteration rather suggest that the Mirdita ophiolite is an analogue of intermediate spreading oceanic lithosphere at a present-day mid-ocean ridge (Ma and Cochran, 1997; Cochran and Sempere, 1997; Sempere and Cochran, 1997).

Acknowledgments

The helpful review of G.Piccardo and J.Bebien is gratefully acknowledged.

This work was supported by Genoa University 95-96 funds to L. Cortesogno, by Pisa University 96-97 funds to P.Elter, and by C.N.R. funds, provided by Centro di Studio per la Geologia Strutturale e Dinamica dell’Appennino and by the Mirdita Ophiolite Project.

REFERENCES

Alexander R.J. and Harper G.D., 1992. The Josephine ophiolite: an ancient analogue for slow- to intermediate-spreading oceanic ridges. In: Parsons, L.M., Murton, B.J., and Browning, P. (Eds.), Ophiolites and their modern oceanic analogues. Geol. Soc. Spec. Publ. London, 60: 3-38.

Aubouin J., Blanchet R., Cadet P., Celet P., Charvet J., Chorovic J., Cousin M., and Rampnoux J., 1970. Essai sur la géologie des Dinarides. Bull. Soc. Géol. France, 12: 1060-1095.

Aubouin J. and Ndojaj I., 1964. Regard sur la géologie et sa place dans la géologie des Dinarides. Bull. Soc. Géol. France, 7: 593-625.

Beccaluva L., Coltorti M., Premti I., Saccani E., Siena F. and Zeda O., 1994. Mid-ocean ridge and supra-subduction affinities in ophiolitic belts from Albania. Ofioliti, Special Issue on “Albanian ophiolites: state of the art and perspectives” (Beccaluva Ed.), 19: 77-96.

Beccaluva L., Di Girolamo P., Macciotta G. and Morra V., 1983. Magma affinities and fractionation trends in ophiolites. Ofioliti, 8: 307-324.

Bortolotti V., Kodra A., Marroni M., Mustafa F., Pandolfi L., Principi G. and Saccani E., 1996. Geology and petrology of the ophiolitic sequences in the Mirdita region, northern Albania. Ofioliti , 21: 3-20.

Boudier F. and Nicolas A., 1977. Structural control on partial melting in the Lanzo peridotites. in: Dept. Geol. Mineral. Ind., 96: 63-78.

Boudier F. and Nicolas A., 1985. Hazburgites and Lherzolites subtypes in ophiolitic and oceanic environments. Earth and Planet. Sci. Lett., 76: 84-92.

Boudier F., Meshi A. and Nicolas A., 1997. The Mirdita ophiolite (Albania): Tethyan Early Jurassic slow - spreading. Terra Nova, 9: 516.

Cannat M. and Lécuyer Ch., 1991. Ephemeral magma chambers in the Trinity peridotite, northern California., Tectonophysics, 186, 3/4: 313-328.

Carosi R., Cortesogno L., Gaggero L. and Marroni M., 1996. Geological and petrological features of the metamorphic sole from the Mirdita ophiolites, Albania. Ofioliti, 21: 21-40.

Ceuleneer G. and Rabinowicz M., 1992. Mantle flow and melt migration beneath oceanic ridges: models derived from observations in ophiolites. Geophys. Monograph 71 “Mantle flow and melt generation at mid-ocean ridges”, Morgan J.P., Blackman D.K., Sinton J.M. Editors, AGU: 123-154

Cochran J.R. and Sempere J.C., 1997. The Southeast Indian Ridge between 88 degrees E and 118 degrees E: gravity anomalies and crustal accretion at intermediate spreading rates. Jour. Geophys. Res., 102, B7: 15462-15487.

Cortesogno L. and Lucchetti G., 1982. Il metamorphismo oceanico nei gabbri ofiolitici dell’Appennino Ligure: aspetti mineralogici e paragenetici. Rend. SIMP., 32/2: 561-579.

Coleman R.G., 1977. Ophiolites - Ancient oceanic lithosphere? Springer Verlag, Minerals and Rocks, 12, 229 pp.

Flinn D., 1996. The Shetland Ophiolite Complex: field evidence for the intrusive emplacement of the “cumulate” layers. Scottish Jour. Geol., 32/2: 151-158.

Franzini M., Leoni L. and Saitta M., 1975. Revisione di una metologia analitica per fluorescenza-X basata sulla correzione completa degli effetti di matrice. Rend. Soc. It. Miner. Petrol. 31: 365-378.

Gaggero L. and Cortesogno L., 1997. Metamorphic evolution of oceanic gabbros: recrystallization from subsolidus to hydrothermal conditions in the MARK area (ODP Leg 153). Lithos, 40: 105-131.

ISPGJ-IGJN, 1982. Gjeologjia e RPSSH. MMKS, Tirana, Albania.

ISPGJ-IGJN, 1983. Harta Gjeologjike e RPSSH, 1:200.000 scale. MMKS, Tirana, Albania.

ISPGJ-IGJN, 1990. Gjeologjia e RPSSH. MMKS, Tirana, Albania.

Karson J.A. and Dick, H.J.B., 1983. Tectonics of ridge-transform intersections at the Kane fracture zone. Mar. Geophys. Res., 6: 51-98.

Karson J.A. and Winters, A.T., 1992. Along axis variations in tectonic extension and accomodation zones in the MARK area, Mid-Atlantic Ridge 23°N. In: Parsons, L.M., Murton, B.J., and Browning, P. (Eds.), Ophiolites and their modern oceanic analogues. Geol. Soc. Spec. Publ. London, 60: 107-116.

Karson J.A., Thompson D.G., Humphris S.E., Edmond, J.M., Bryan, W.B., Brown, J.R., Winters, A.T., Pockalny, R.A., Casey, J.F., Campbell, A.C., Klinkhammer, G., Palmer, M.R., Kinzler, R.J. and Sulanowska, M.M., 1987. Along axis variations in tectonic extension and accomodation zones in the MARK area. Nature, 328: 681-685.

Kelemen P.B., Hirth G., Shimizu N., Spiegelman M. and Dick H.J.B., 1997. Review of melt migration processes - the adiabatically upwelling mantle beneath oceanic spreading ridges. Phil. Trans. Royal Soc. London Ser.A. 355/1723, 283-318.

Leoni L. and Saitta M., 1975. X-ray fluorescence analysis of 29 trace elements in rocks and mineral standards. Rend. Soc. It. Miner. Petrol. 32: 497-510.

Ma L.Y. and Cochran J.R., 1997. Bathymetric roughness of the Southeast Indian Ridge: implications for crustal accretion at in-

termediate spreading rate mid-ocean ridges. Jour. Geophys. Res., 102, B8: 17697-17711.
Madge L.S. and Sparks D.W., 1997. Three-dimensional mantle upwelling, melt generation, and melt migration beneath segment slow spreading ridges. Jour. Geophys. Res., 102, B9, 20571-20583.
Marcucci M. and Prela M., 1996. The Lumi zi (Puke) section of the Kalur Cherts: radiolarian assemblages and comparison with other sections in northern Albania. Ofioliti, 21: 71-76.
Nicolas A., 1988. Structures of ophiolites and dynamics of oceanic lithosphere. Kluwer Academic Publisher, 4, 367 pp.
Pearce J.A., and Parkinson L.J. 1993. Magmatic processes and plate tectonics. In: H.M. Prichard, T. Alabaster and N.B.W. Harris, C.R. (Eds.), Magmatic Processes and Plate Tectonics. Geol. Soc. London Spec. Publ., 76, 373-403.
Quick J.E., 1981. The origin and significance of large, tabular dunite bodies in the Trinity peridotite, Northern California, Contrib. Mineral. Petrol., 78: 413-422.
Robertson A.H.F. and Dixon J.E., 1984. Introduction: aspects of the geological evolution of the Eastern Mediterranean. Dixon J.E. and Robertson A.H.F. (Eds.), The Geological evolution of the Eastern Mediterranean. Geol. Soc. of London, Spec. Pubbl., 17: 1 - 73.
Sempere J.C. and Cochran J.R., 1997. The Southeast Indian Ridge between 88 degrees E and 118 degrees E: variations incrustal accretion at constant spreading rate. Jour. Geophys. Res., 102, B7: 15489-15505.
Shallo M., 1991. Ophiolitic melange and flyschoidal sediment of the Tithonian - Lower Cretaceous in Albania. Terra Nova, 2: 476-483.
Shallo M., 1992. Geological evolution of the Albanian ophiolites and their platform periphery. Geolog. Rund. 81/3: 681-694.
Shallo M., 1994. Outline of the Albanian Ophiolites. Ofioliti, Special Issue on “Albanian ophiolites: state of the art and perspectives” (Beccaluva Ed.), 19: 57-75.
Shallo M., Kote D. and Vranai A., 1987. Geochemistry of the volcanics from ophiolitic belts of Albanides. Ofioliti, 12: 125-136.
Spray J.G., Bébien J., Rex D.C. and Roddick J.C., 1984. Age constraints on the igneous and metamorphic evolution of the Hellenic-Dinaric ophiolites. In: Dixon J.E. and Robertson A.H.F. (Eds.), The Geological evolution of the Eastern Mediterranean. Geol. Soc. London, Spec. Pubbl., 17: 619-628.
Varga R.J. and Moores E.M., 1985. Spreading structure of the Troodos ophiolite, Cyprus. Geology, 13: 846-850.

Receveid, July 27, 1998
Accepted, November 2, 1998